We are IntechOpen, the world's leading publisher of Open Access books Built by scientists, for scientists

4,800
Open access books available

122,000
International authors and editors

135M
Downloads

Our authors are among the

154
Countries delivered to

TOP 1%
most cited scientists

12.2%
Contributors from top 500 universities

CLARIVATE ANALYTICS BOOK CITATION INDEX INDEXED

WEB OF SCIENCE™

Selection of our books indexed in the Book Citation Index in Web of Science™ Core Collection (BKCI)

Interested in publishing with us?
Contact book.department@intechopen.com

Numbers displayed above are based on latest data collected.
For more information visit www.intechopen.com

Chapter

Biomedical Applications of Nanomaterials: Nanotubes and Metal-Organic Frameworks (MOFs)

Miguel Martell-Mendoza, Cuauhtémoc Pérez-González, Hiram I. Beltrán, Roberto Serrano-Vega and Carlos Alberto Méndez-Cuesta

Abstract

Nanomedicine plays an important role in the diagnosis, treatment, monitoring and control of biological systems in the area of nanotechnology and has been referred by the National Institute of Health (NIH) as an emergent way of medicine. Nanoparticles are new delivery vehicles with the ability to release drugs to a specific cell type or tissue, which may also improve the pharmacological activity of those drugs by controlling their release, as well as prolonging their short half-lives in blood. The aim of this review is to gather several options of MOFs and nanotubes synthesised with different nanoparticles and processes, some including compound loading and release studies, with particular focus on 13 anti-cancer compounds e.g. doxorubicin, curcumin, methotrexate, etc.; 3 anti-inflammatory compounds, namely ibuprofen, salicylic acid and chlorogenic acid; and with 5 miscellaneous bioactive compounds, including rifampicin, griseofulvin, enoxacin, etc. Finally, other biomedical applications for these composites are shown, like being enzyme immobilisation agents, for water treatment e.g. in swimming pools, and other becoming support to carry & secure integrity of drugs.

Keywords: nano MOFs, nanotubes, drug delivery, biomedical applications, composite materials

1. Introduction

Any material could be described as a (semi) solid entity, substance or device that things could be made from, with the purpose to resolve a present or future need. There are a lot of daily examples that we are able define as materials, for instance, cloth, wood and electronic devices, such as computers, cell phones and smart TVs. Materials could be divided into natural and synthetic groups and, at the same time, they are commonly classified depending on their composition or physicochemical properties. Nowadays, the search for synthetic materials has been fast growing, because of their electrical, thermal, mechanical, structural and in many cases, their emergent properties, that make them suitable for many fields of science.

In recent years, the development and modification of materials at the nanoscale for biomedical purposes has been extensively reported in the literature. One of the most significant of these has been the encapsulation or capture of drugs with the purpose of increasing dosage, providing protection against body's metabolism and directing the drug to the therapeutic target or a specific site. Despite these benefits, the principal limitations include the host-guest compatibility, very closely related with toxicity, the degradation and the half-life of the nanomaterial. For this reason, these side studies should be included when a new material is developed for biomedical purposes.

Metal Organic Frameworks (MOFs) are a class of microporous 1D, 2D or 3D crystalline materials, constructed from a metal ion held together by organic polyfunctional ligands, that confer special characteristics to this arrangement. Some of these features are their high/tunable surface area, homogenous porosity, their great stability and crystallinity, among other. Due to these characteristics, MOFs are widely applied in the storage and separation of gases, as sensors, and in matrices to capture/deliver a large amount of several kinds of molecules and in particular drugs even showing specificity towards therapeutic targets and thus improving the effect of the drugs and their bioavailability.

Besides, nanotubes have the potential to revolutionise biomedical research, due to their important electrical, chemical, thermal, mechanical and structural properties which have made them an area of great research interest. With this in mind, they are capable to display metallic, semiconducting and superconducting electron transport properties. Although carbon nanotubes (CNTs) are the most common, they also could be constructed from peptides and organometallic moieties or materials. The CNTs could be used in numerous applications, including nanofluidic systems, biopharmaceutical applications such as drug delivery, implantable biomedical devices, diagnostic tools and devices in radiation oncology, biosensors, probes and quantum dots, such as nanosensors and nanorobots and also for tissue engineering applications [1].

Hence, the gathering criteria of all these research examples in this chapter is focused on evidencing some of the most relevant examples from the last 5 years (2014–2018) in terms of nanomaterials, with capability to act as (i) drug delivery systems and for (ii) general biomedical applications, addressing aspects such as the composition of these materials, type of loaded/tested/delivered drugs interacting with both, (nano) MOFs or nanotube materials and their perspectives on the synthesis and modification of these new composites for such applicability.

2. Drug delivery

2.1 Anti-cancer

In this first contribution, the MIL-100(Fe) was prepared using a hydrothermal microwave-assisted method. Synthetic procedure required a mixture of $FeCl_3$ hexahydrate and 1,3,5-benzenetricarboxylic acid settled in deionised water, which was heated at 130°C during a period of 6 min. The characterisation of the crystalline substance was performed by X-ray powder diffraction (XRPD), meanwhile particle size and morphology were determined by Dynamic Light Scattering (DLS) and Transmission Electron Microscopy (TEM). Additionally, surface morphology was characterised using Field-Emission Scanning Electron Microscopy (FESEM) and the pore size was determined by nitrogen sorption experiments. The measured Langmuir surface was of 1350 ± 100 $m^2 g^{-1}$. The pore size of this material measured a free diameter of *ca.* 25 and 29 Å, which is accessible through the pentagonal and

hexagonal microporous windows present in this material (5.5 and 8.6 Å). The incorporation of doxorubicin (DOXO) in MIL-100(Fe) was determined by UV-Vis, circular dichroism (CD) and fluorescence spectroscopies, and the determined concentration of DOXO present in this material was 9 wt% (**Figure 1**) [2].

In this other piece of work, Gemcitabine-5′-monophosphate (Gem-MP) was appropriately loaded into MIL-100(Fe) MOF material, reaching a top concentration of 30.7 ± 0.8 wt%; this was confirmed by High Performance Liquid Chromatography (HPLC) and radioactivity counting methods (**Figure 2**). The Gem-MP@MIL-100(Fe) release studies were performed in PBS media and 100% of release of this drug molecule was reached at 4 h. The Half Maximal Inhibitory Concentration (IC_{50}) of both empty and loaded materials were tested in pancreatic cancer cell lines (PANC-1) using the MTT method. This experiment has shown that the unloaded material had no effect on the viability of cells. However, when Gem-MP and Gem-MP@MIL-100(Fe) were tested, the IC_{50} were 17.5 μM and 45 nM, respectively. This finding clearly confirmed that the activity of Gem-MP is improved *ca.* 389 times when it is loaded into MIL-100(Fe) material [3].

Moreover, a phytochemical-ligand-containing metal-organic framework of the formula $\{[Zn_2(fer)_2]\}n$, (Zn-fer MOF) was prepared, where the organic ligand named H_2fer = ferulic acid, and its structural elucidation revealed the presence of large nanocage-based pores suitable for ionic or molecular guest incorporation. With the latter in mind, Zn-fer MOF was employed as interaction matrix for the adsorption and *in vitro* carriage of 5-fluorouracil (5-FU), obtaining 5-FU@Zn-fer material. The ability of 5-FU@Zn-fer to deliver 5-FU, biodegradation and cytotoxicity assays were also determined. Additionally, the grand canonical ensemble Monte Carlo (GCMC) simulation was performed to *in silico* investigate the loading of 5-FU to Zn-fer at the molecular level. With these results, authors determined that 5-FU could be adsorbed into this BioMOF with a high loading. GCMC simulations validated the experimental trend, showing that 5-FU could be incorporated into desolvated Zn-fer MOF reaching loadings as high as 0.388 g g^{-1}. The analysis of radial distribution function (RDF) and configuration snapshot analysis, showed that the most important interaction between 5-FU and Zn-fer MOF are hydrogen bonding and dipolar interactions (**Figure 3**). Furthermore, the delivery of 5-FU occurred within 100 h and at that time, 99% of the loaded drug was already released. For further sights, this may lead to the desired modulated release of anti-cancer agents over a long-time and probably reducing side-effects for patients. Finally, according

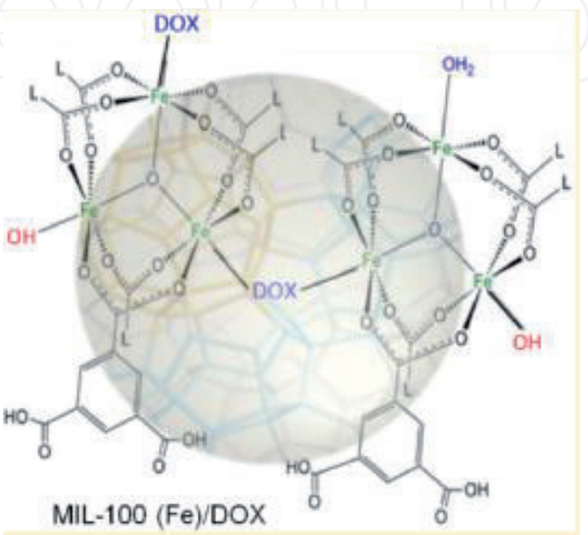

Figure 1.
MIL-100 (Fe)/DOX [2].

Figure 2.
Representation of Gem-MP encapsulation into MIL-100(Fe) [3].

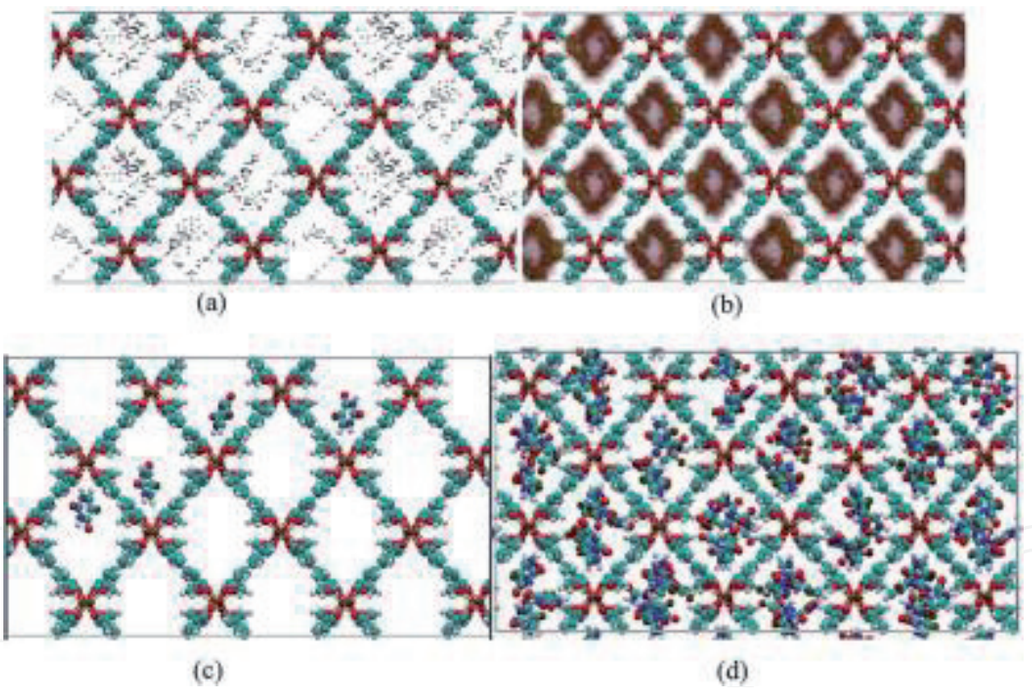

Figure 3.
The density of 5-FU under 10-5 mPa, 1 mPa for (a) and (b) (top pictures) and the snapshot of 5-FU in Znfer-MOF for (c) and (d) (down pictures) [4].

to our criteria, this investigation has provided impetus to design and develop similar structured biocompatible MOFs which are able to offer relatively superior drug carrying and drug release properties [4].

Some other investigation aims for the incorporation of target molecules based on a multistep post-functionalization procedure. In the cited research, the authors report a novel approach combining MOF synthesis and molecule encapsulation in a one-pot process. Researchers have therein demonstrated that large molecules are appropriate to be entrapment in the composite zeolitic imidazolate framework (ZIF). The distribution was homogeneous into the ZIF, and in this way their

loadings could be improvement. The ZIF-8 crystals were carried with DOXO to obtain DOXO@ZIF-8 composites, like efficient drug delivery vehicles for cancer therapy using pH-dependent release (**Figure 4**). The DOXO@ZIF-8 showed higher efficiency than DOXO against breast cancer cell lines, due to well-known composite enhancements. This one-pot process opens new possibilities to construct multifunctional delivery systems for a wide range of applications [5].

The incorporation of drugs in biodegradable polymeric particles is one of many processes that controllably and significantly increase their release and action. The synthesis and physicochemical characterisation of ZnBDC-MOF (MOF-5) + DOXO giving place to DOXO@ZnBDC hybrid, and the effectiveness of this composite in the sustained release of the DOXO drug has been described. In a first procedure, the MOF-5 was obtained by mixing sodium terephthalate (Na_2BDC), $Zn(NO_3)_2{\cdot}6H_2O$ and H_2O; the suspension was then transferred to a CEM (Microwave reactor) S-Class System with vessel temperature set at 120°C. The loading of DOXO into MOF-5 was performed by stirring 0.034 g of the dehydrated MOF-5 powder in 4 mL of aqueous solution containing 0.1 g of DOXO during 1 day interaction period. An experimental and theoretical study is presented of the interaction between the MOF-5 material and DOXO molecule (**Figure 5**). The synthesis was carried on, and the resulting material was characterised by elemental analysis and XRPD. The experimental incorporation was accomplished and analysed by Fourier Transform Infrared Spectroscopy (FTIR) and UV-Vis spectroscopies, as well as by XRPD. An analysis of the adsorption of the DOXO@ZnBDC system confirmed the successful incorporation of the drug, revealing 0.0163 g of DOXO included into the composite, or an equivalent to 96% of the drug. The stability and drug release profile of DOXO@ZnBDC confirmed that the system released DOXO in a sustained or bimodal manner, like other systems, releasing 51.4% of the DOXO molecule in 48 h. The behaviour described in the article demonstrates that the DOXO@ZnBDC system has the potential against cytotoxic cancer cell lines NCI-H292 (human pulmonary mucoepidermoid carcinoma), HT-29 (human colorectal adenocarcinoma) and MCF-7 (human breast adenocarcinoma). The cytotoxic effect, an intensity scale for the cytotoxic potential of the system under study, was as stated in the following tendency related to cell growth inhibition [CGI], zero activity, ranging from 1 to 20%; little activity, 20–50%; moderate activity, 50–70%; and significant activity, 70–100%. *In vitro* cytotoxicity of unloaded MOF-5 was HT29 CGI = 72.6%, MCF-7 CGI = 47.4%, NCI-H-292 CGI = 77.0%; for free DOXO, HT29 CGI = 57.0%, MCF-7 CGI = 55.2%, NCI-H-292 CGI = 76.3%; and for DOXO@ZnBDC was HT29 CGI = 70.7%; MCF-7 CGI = 20.1%; NCI-H-292 CGI = 26.4% at different

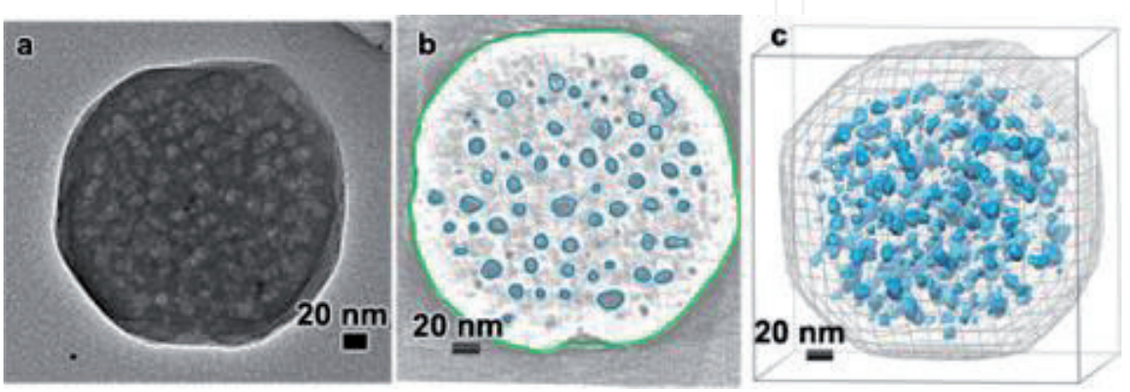

Figure 4.
Distribution of mesopores in DOX@ZIF-8 particles illustrated by electron tomography. (a) TEM image of a DOX@ZIF-8 single crystal. (b) Cross-section of the electron tomogram with the mesopores marked by blue lines. (c) 3D distribution of the mesopores in the DOX@ZIF-8 particles [5].

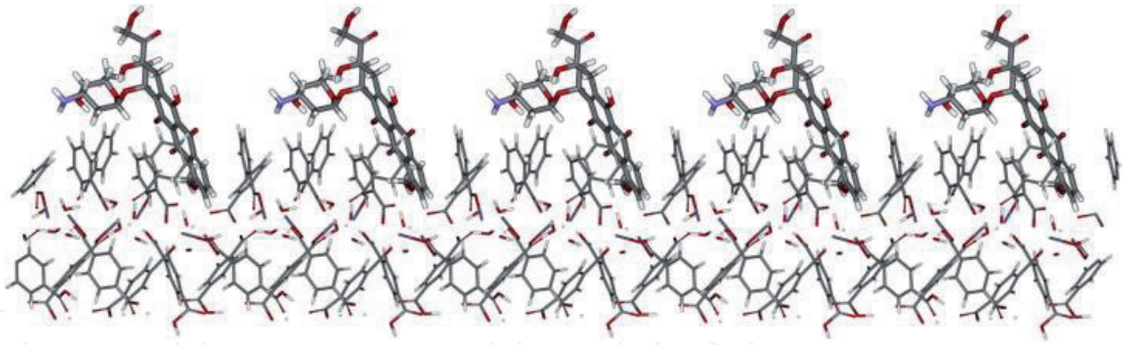

Figure 5.
Simulated adsorption of the DOXO in surface of MOF by means of PM6 calculation [6].

concentrations after 72 h. As can be seen, the MCF-7 & NCI-H-292 proved to be the most sensitive strains, because of the activity of composite material [6].

Another work of ZIF-8 crystal as a functional material was used to control the release of an autophagy inhibitor, 3-methyladenine (3-MA), and avoid the decomposition of large quantities of the drug and enhance their bioavailability (**Figure 6**). The HeLa cells treated with 3-MA@ZIF-8 NPs has shown that the autophagosome development was successfully blocked. The pH-sensitive dissociation rises the efficiency of autophagy inhibition at the same concentration of 3-MA. *In vivo* test data showed higher efficacy to repress the expression of autophagy-related markers, Beclin 1 and LC3, in 3-MA@ZIF-8 NPs more than free 3-MA. Some of the most important features underlined by the authors is that ZIF-8 resulted an efficient drug delivery vehicle in antitumor therapy, especially in inhibiting autophagy of cancer cells. The cytotoxicity of 3-MA@ZIF-8 nanoparticles was evaluated by determining cellular viability through an MTT assay. The 3-MA@ZIF-8 NPs system was found to be toxic to HeLa cells in a dose-dependent manner, after treatment at a concentration of 7.5 μg mL^{-1} (equivalent to a concentration of 3-MA of 1.5 μg mL^{-1}) for 24 h. The values were even lower after the cells had been treated with 3-MA@ZIF-8 NPs at a concentration of 10 μg mL^{-1} [7].

Following the versatility of ZIF-8 system, in other studies, DOXO was loaded into this MOF via a one pot process. The *in situ* loading process implied the water dissolution of the DOXO bioactive at 4 mg mL^{-1}, then 0.2 g (0.66 mmol) of $Zn(NO_3)_2{\cdot}6H_2O$ were dissolved in 0.8 mL of water, into which 4 mL of DOXO solution was added. After that 2 g of 2-methylimidazole were dissolved in 8 mL water and this was slowly dropped into the previous mixture. The *in situ* assembled DOXO@ZIF-8 composite was then coated with polydopamine, successively chelated with Fe^{3+} and conjugated with hyaluronic acid (HA). Finally, all these resulted in a multifunctional ZIF-8 nanocarrier of DOXO@ZIF@HA nature (**Figure 7**). The

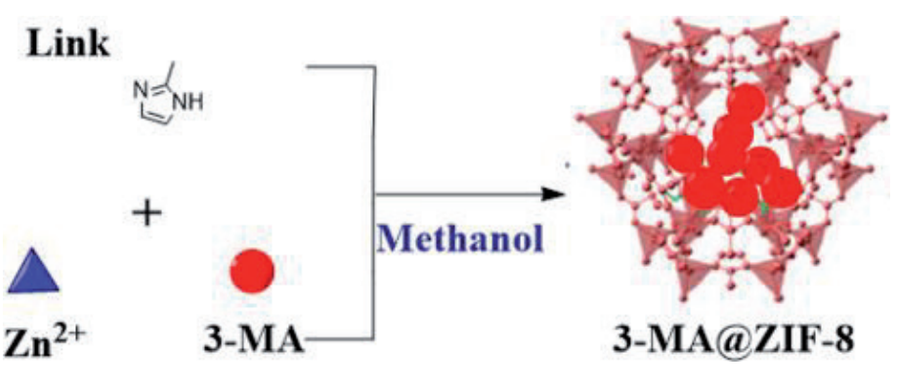

Figure 6.
Schematic representation of 3-MA@ZIF-8 [7].

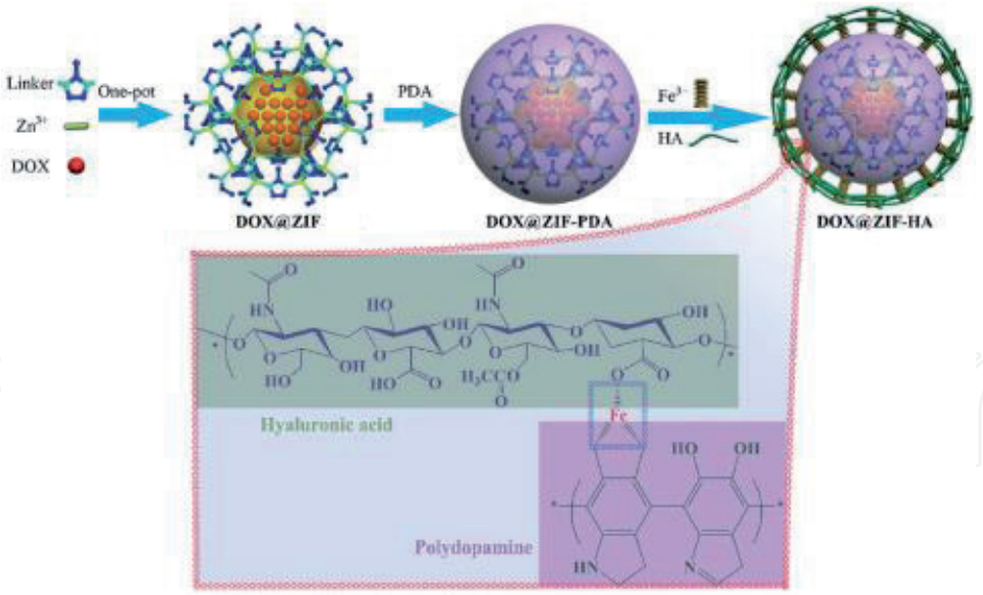

Figure 7.
Diagram for the preparation of DOX@ZIF-HA and the Fe^{3+}-mediated coordination interaction between HA and PDA [8].

characterisation results confirmed the successful formation of the hybrid nanocarrier. The loading efficacy was determined to be 8.92 ± 0.53%. The data suggest that the release of DOXO from the nanocarrier demonstrated a sustained nature, but in this case regardless of the pH value. The cumulative amount of DOXO released at pH 5.0 and 7.4 was 70.1 and 9.8%, respectively, clearly showing a pH dependent behavior. The results of flow cytometry and confocal laser scanning microscope shown the targeting ability of DOXO@ZIF-HA towards prostate cancer PC-3 cells. In order to make notice the effect of composite assembly, the therapeutic efficacy of DOXO@ZIF-HA was clearly improved when compared with free DOXO. The cells were treated with different formulations of free DOXO and DOXO@ZIF-HA for 24 h and untreated cells were used as a control. At a DOXO concentration of 1 mg mL^{-1}, the cell viability for free DOXO and DOXO@ZIF-HA was 65.61 and 48.59%, respectively. This is mainly since the efficient internalisation of the targeted carrier DOXO@ZIF-HA could improve the intracellular DOXO concentration. Hence, authors state that the constructed ZIF-8 based multifunctional nanocarrier could be a candidate for cancer theranostics [8].

Another method to effectively carry DOXO to the breast cancer sites is the use of halloysite nanotubes (HNTs) coated with poly(ethylene glycol) (PEG) and folate (HNTs-PEG-FA), which have been used as drug delivery systems. The HNTs were reduced to ~200 nm by ultrasonic scission and then functionalised with N-hydroxylsuccinimide-polyethylene glycol carboxylic acid (NHS-PEG-COOH) and folate (FA) moieties. The DOXO@HNTs-PEG-FA was prepared by filling with DOXO on HNTs-PEG-FA via physical adsorption (**Figure 8**). The maximum release of DOXO from DOXO@HNTs-PEG-FA was reached to 35 h at pH 5.3. The DOXO@HNTs-PEG-FA ensemble showed significant inhibition of proliferation and induction of apoptosis in MCF-7 cells with positive FA receptors but this is not true for L02 cells without FA receptors. The *in vivo* anti-breast cancer activity of DOXO@HNTs-PEG-FA was confirmed using 4T1-bearing mice. The DOXO@HNTs-PEG-FA reduced toxicity and inhibited tumour growth associated with higher levels of caspase-3 protein. These results suggest that FA-conjugated HNTs may be designed to be a novel drug delivery system for targeted therapy of breast cancer via intravenous [9].

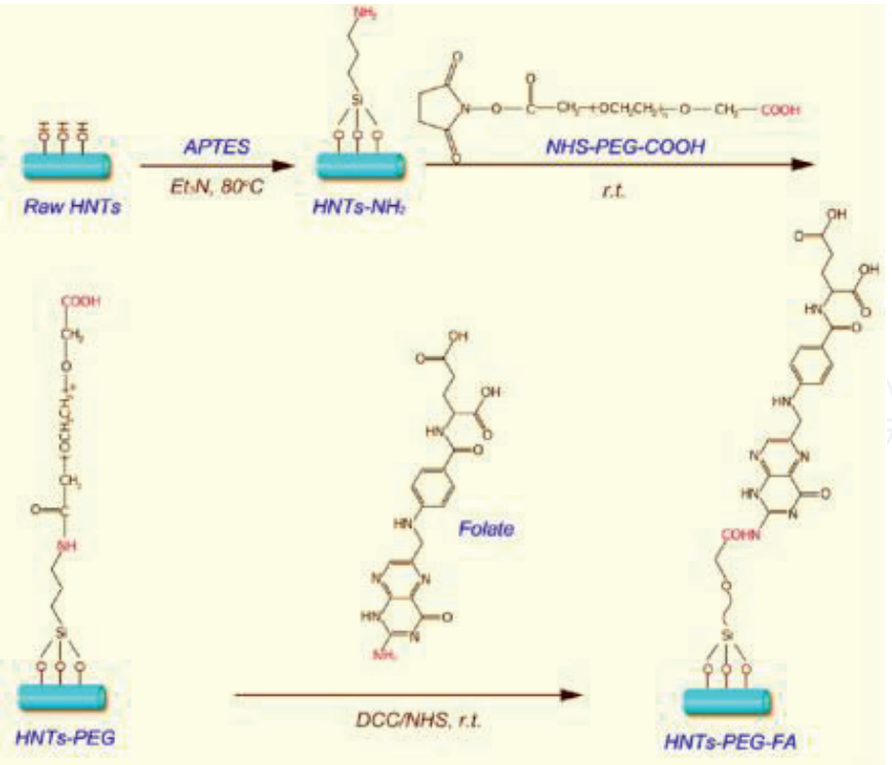

Figure 8.
Schematic representation of HNTs-PEG-FA preparation [9].

Another drug delivery strategy is when some peptides were used in the synthesis of nanotubes capable of this method of carrying. Nanotubes was synthetized using two dipeptides based on their flexibility, one of them using the Phe-Phe backbone (βPhe-Phe and βPhe-ΔPhe); containing βPhe amino acid, and the other containing βPhe like a backbone constraining ΔPhe (α,β-dehydrophenylalanine) amino acid. Both were characterised by X-ray diffraction, DLS, TEM, FTIR and CD. Small drugs like riboflavin, DOXO, chloramphenicol and chloroquine, were tested in encapsulation experiments in these new nanotubes. The results have shown comparable encapsulation in both types of nanotubes, and the loaded contents were 7, 15, 35 and 18%, respectively. Moreover, these dipeptides have not shown cytotoxicity towards HeLa (cervical uterine cancer), B6F10 (melanoma mouse) and L-929 (fibroblast mouse) cells with different concentrations of peptide nanostructure. Mitoxantrone free and encapsulated in βPhe-Phe and βPhe-Phe/βPhe-ΔPhe nanotubes was tested in equals amounts against cell lines HeLa and B6F10. The viability of HeLa cells treated with free mitoxantrone at 3 mg mL^{-1} was 77%, while when encapsulated in βPhe-Phe or βPhe-ΔPhe nanotubes, the viability reduced to 58 and 53%, respectively. However, the value of viability for B6F10 cells changed from 85 to 60% and 31%, respectively. These results suggest that administration of mitoxantrone with dipeptide nanotubes was more effective against HeLa and B6F10 cancerous cells [10].

There are reports that by combining the advantage of multi-walled carbon nanotubes (MWCNTs) and interpolymer supramolecular complexes, a new carrier system consisting of poly (acrylic acid)/PEG/carbon nanotubes (PAA/PEG/CNT) has been assembled. The oxidised MWCNTs were obtained with nitric acid treatment, yielding HOOC-MWCNTs, and then submitted to an activation reaction with $SOCl_2$ to get MWCNT-COCl. The PEGylation of acyl chloride groups on the oxidised MWCNTs was completed by refluxing with PEG4000 and subsequently complexing with the second polymer (PAA). Then, methotrexate (MTX) and

cyclophosphamide (CPP) were loaded on PAA/PEG/CNT, and nanoparticles were characterised by FTIR, SEM, TGA and NMR. The efficiency of loaded drugs was determinate, an *in vitro* drug release study was carried out with UV spectroscopy in buffer human body (pH = 7.4) and buffer at pH of cancer cells (pH = 4). The *in vitro* release of drugs from nanoparticles showed an initial burst release followed by sustained release, this fact was due to the presence of the drug on the surface of the nanoparticles. The rate of release at this stage was very high and after 1 h, the drug concentration was constant [11].

Another kind of composite is based in the synthesis of the bio-compatible polymer PEG-400 and MWCNTs. The MWCNTs were PEG-400-broken-assisted into small tubes by vortex mechanical mixing with tungsten-carbide balls for about 15 h. Length separation of MWCNTs was then carried out using differential centrifugation also PEG-400-assisted with various concentrations of the polyether. Novel cocoon nanoparticles of sizes ranging about 100–200 nm were observed in one of the centrifuged fractions. The cocoon pellets were re-dispersed in water using ultrasonication for 2 min and characterised using Field Emission SEM, TEM and FTIR. Energy Dispersive Spectroscopy (EDS) and diffraction patterns were also obtained using TEM. Curcumin (CUR) was added as the bioactive, anticancer drug, to these cocoons, and it was observed that it was distributed in these motifs while it was not attached to the CNT-PEG solution without cocoon structures (**Figure 9**). The cocoon and CUR@cocoon samples exhibited much lower haemolysis than CUR alone, with a value of 0.04, 0.03 and 0.09%, respectively. Also, it was observed that all cocoon and CUR@cocoon samples were non-toxic at the concentrations tested. The cell viability of CUR@cocoon samples were less than 95% at 50 μg, indicating cytotoxicity on L-929 cells at higher concentrations. The CUR@cocoon assemblies were dispersible in saline solution and could be internalised by brain cancer cells (C6 glioma), while free CUR dispersed in saline solution could not enter C6 glioma cells, this clearly evidenced differential diffusion and selectivity in this trial [12].

In this work was prepared HNT@CUR-Au/CS NPs by an *in situ* preparation. First, gold, HNTs and CUR were mixed to obtain HNT@CUR-Au and subsequently coating with bio-adhesive chitosan (CS). The HNT@CUR-Au/CS has been characterised by FTIR, XRPD, XPS and STEM methods (**Figure 10**). The loading efficiency of drug into the nanostructures was 12% at most. The release of the drug was more efficient under pH = 5.5 than pH = 7.4. The anticancer potential of HNT@CUR-Au/CS against MCF-7 cells shown more efficient anticancer activity in

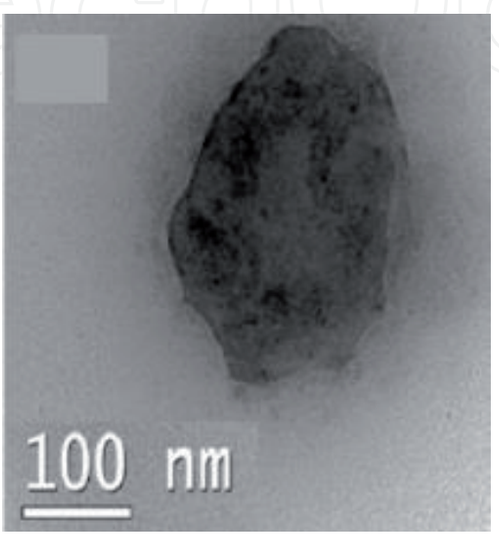

Figure 9.
High resolution TEM of curcumin added to nano-cocoons [12].

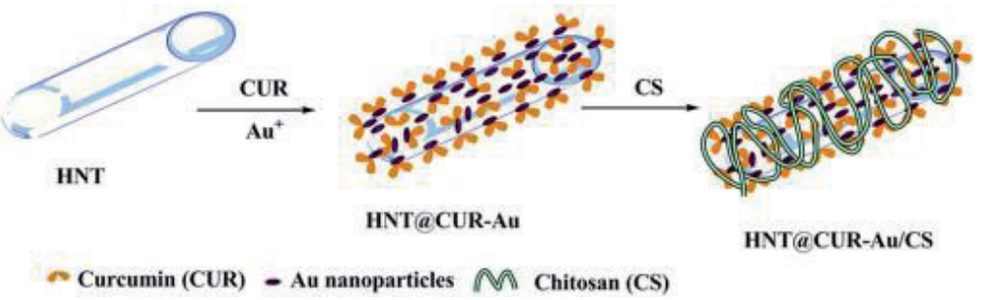

Figure 10.
Schematic representation of formation of HNT@CUR-Au/CS [13].

the intracellular environment than in extracellular conditions, in agreement with their own previous differential pH physicochemical CUR-release tests. Moreover, the development of this composite consisting of Au NPs and pH-responsive CUR release could make it suitable for cancer cell-targeted drug delivery platforms, also with the possibility to develop NIR-imaging [13].

In an another research group, a new design of hydroxypropyl-β-cyclodextrin (HP-β-CD) modified carboxylated single-walled carbon nanotube (CD-SWCNTs) assembly was employed to improve the biocompatibility and reduce the toxicity of the self-carbon nanotubes for the release of the anticancer drug formononetin (FMN). According to the analysis of results developed by the authors related to findings in FTIR, HP-β-CD was successfully grafted into carboxylated single-walled carbon nanotubes (SWCNTs-COOH). The samples were characterised by XRPD, differential scanning calorimetry (DSC), DLS and SEM. The loading of FMN in CD-SWCNTs to develop FMN@CD-SWCNTs system was determined by HPLC. The entrapment efficiency and loading capacity were determinate to be 88.66 ± 3.13% and 8.43 ± 1.11%, respectively. The HP-β-CD system possesses a hydrophobic inner cavity and a hydrophilic exterior, which could bind/inner entrap hydrophobic drug molecules to form stable host-guest supramolecular assemblies. The SWCNTs have a high aspect ratio and surface area, and they could interact with FMN via π-π stacking interactions, which resulted in a high entrapment efficiency (**Figure 11**). The cumulative release of FMN from FMN@CD-SWCNTs nanocarrier achieved 4.11 ± 0.62% within 48 h at a pH = 5.3, compared with 16.75 ± 0.88% when exposed to pH = 7.4. This kind of drug release kinetics demonstrated a slow and sustained release, but in this particular case resulted more efficient at physiologic

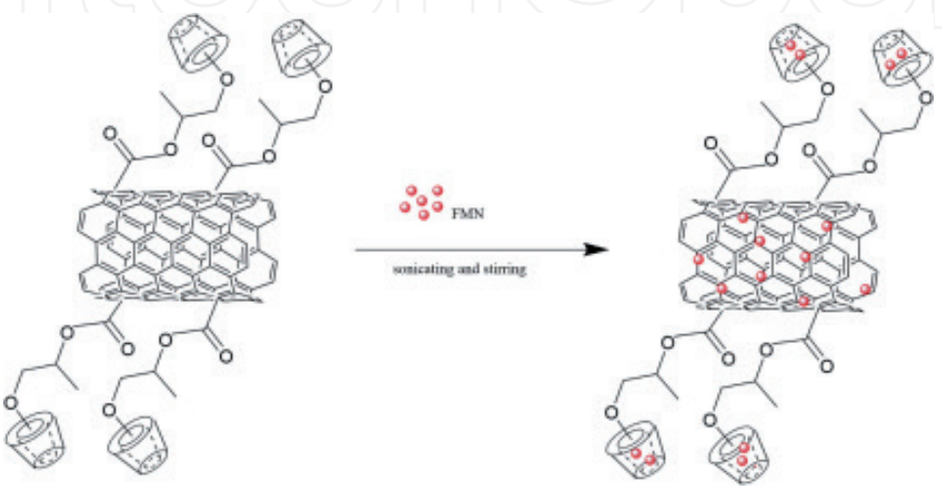

Figure 11.
Scheme of the possible interaction of FMN with CD-SWCNTs [14].

pH, in comparison with other related systems. The *in vitro* cytotoxic activity of FMN@CD-SWCNTs nanocarriers against MCF-7 and HeLa cells was tested by using the WST-1 assay. The antitumour activity of FMN@CD-SWCNTs had an IC_{50} = 17.989 ± 1.255 and 21.775 ± 1.338 μmol L^{-1} for MCF-7 and HeLa cells, respectively. This latter was higher than that of lone FMN with an IC_{50} = 55.986 ± 2.479 and 72.995 ± 0.551 μmol L^{-1} for MCF-7 and HeLa cells, respectively. These results confirm that FMN@CD-SWCNTs complexes exhibit a higher cytotoxic activity than free drug [14].

In this review, f-SWCNTs were used as the starting material to react with the anticancer drug betulinic acid (BA) to produce f-SWCNTs-BA conjugate via π-π stacking interactions. The BA@f-SWCNTs composite was assembled by dispersed f-SWCNT in a solution with BA in methanol and sonicated for 30 min. The BA@f-SWCNTs conjugate was characterised by XRPD, TGA, FE-SEM and FTIR spectroscopy to elucidate and quantify the concentration of the drug in BA@f-SWCNTs and the structure of the conjugate (**Figure 12**). The results indicated that the drug loading capacity was around 20 wt%. The release of the drug from BA@f-SWCNTs was tested in a human body media at pH 7.4 and 4.8 value; this study has shown that the release rate of BA is higher in pH 7.4 than pH 4.8, again another example of controlled release but an higher pH values, and for this reason drug delivery resulted to behave pH-dependent. The maximum percentage release of BA reached 89.2% (24 h) and 78.7% (10 h) when exposed to pH 7.4 and 4.8, respectively. The cytotoxicity assays for BA, f-SWCNT and conjugated BA@f-SWCNTs were performed in a healthy fibroblast cell line (3T3) and two cancer human lines, liver cancer (HepG2) and lung cancer (A549), at various concentrations ranging from 0.78 to 50 μg mL^{-1} at 72 h and were measured by the MTT method. The experiment has shown that at several doses the f-SWCNT did not have a significant impact on the viability of any cell lines. However, at a dose of 25 μg mL^{-1} of BA@f-SWCNTs, the viability of HepG2 and A549 were reduced by more than 50%, in comparison with lone BA that shown low cytotoxicity at the same concentration [15].

Also, there are reports describing the preparation of a biocompatible and pH sensitive biodegradable hydroxyapatite material using mesoporous nanoplates (Hap PNPs) employing a hydrothermal technique with carboxymethylcellulose calcium salt. This material was characterised using FESEM; the length of spindle structures was 20 nm and the diameter was 10 nm on average, the specific area was 180 m^2 g^{-1} and a crystallite size of 17 nm was calculated using the Debye-Scherer equation. This material was tested as a nanocarrier, and the model loaded drugs were MTX and andrographolide. The UV-vis analysis confirmed that the HAp PNPs have a drug loading efficiency of 50–55.5% at pH = 7.0, which is greater than the conventional HAp nanostructure loading capacity, showing a sustained release at a pH = 4.4. The andrographolide anticancer drug was readily loaded onto prepared HAp PNPs and released in a pH-controlled manner, where for an acidic pH = 4.4

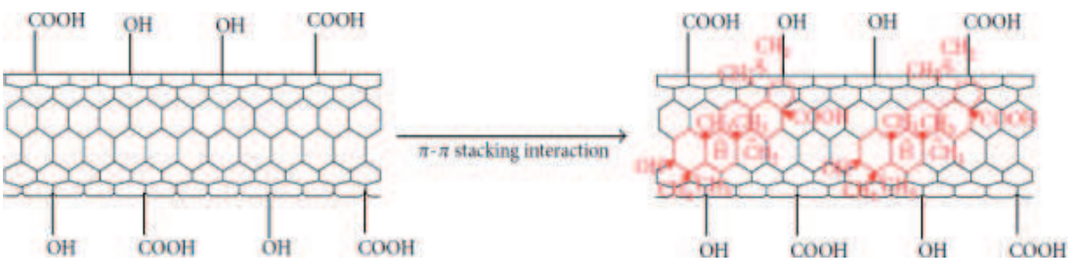

Figure 12.
Scheme for the functionalization of BA molecule onto the f-SWCNTs nanocarrier via π-π stacking interaction [15].

the liberation is higher as compared with a pH of 7.0 or 9.0. The MTT assay was used for the determination of the cytotoxicity in A431 cell lines at different doses of HAp PNPs (0–1000 μg mL^{-1}) and andrographolide loaded (25, 50, 75, 100, 125 and 150 μM) on HAp PNPs (fixed concentration of 100 μg mL^{-1}) at different pHs of 9.0, 7.0 and 4.4 for 24 h. The results have shown that the prepared HAp PNPs exhibited biocompatibility at higher doses of 1000 μg mL^{-1}. Also, they demonstrated that the cytotoxic effect increased by increasing the dose of andrographolide loaded HAp PNPs at pH = 9.0 with an IC_{50} = 125 μM [16].

In the next work nanotubes of SiO_2 were prepared with a uniform diameter of 2.5 nm and shell thickness of 1–5 nm and the exterior surface was silane functionalised and had a negative charge; hence could be selectively loaded with compounds positively charges. The synthesis was carried out using (3-chloropropyl) trimethoxysilane (CPTMS) and tetraethylorthosilicate (TEOS). The characterisation was performed with TEM, X-ray spectroscopy elemental mapping and the particle size was determined by dynamic analysis. The concentration of organic material was quantified using FTIR. This material had a transmittance of aprox. 84% at 550 nm. The load of organic material was 63.6% and determinate by TGA. Positively charged DOXO was loaded in the material; 80% of material was released over 2 weeks, due to size of the elongated nanochannel that suppressed the diffusion [17].

2.2 Anti-inflammatory

Other method to prepare porous MOF materials is the union of an organic linker with other secondary building unit (SBU). For example $[M_2(COO)_4]$ (M = Cu, Zn, Mn, Ni, etc.), $[M_3O(COO)_6]$ (M = Fe, Ni, etc.), $[Zn_4O(COO)_6]$ and $[M_6O_4(OH)_4(COO)_{12}]$ (M = Zr, Hf) MOF systems. Calcium ion possess acid properties, large atom radii and large coordination number, for these reasons is not frequently found it in MOFs structures in comparation with other transition metal-based MOFs. However, the assembly of calcium ions with a big triangle aromatic carboxylic acid ligand has been reported and resulted in a unique porous Ca-MOF structure with nano-sized $\{Ca_{11}\}$ carboxylate SBU and a 2D square channel with a size of 10.8 Å × 10.7 Å. The crystal structure was solved by single crystal X-ray diffraction methods. To determine the thermal stability of the material TGA method was used, where it was found that a continuous slow weight loss was observed until 550°C, the authors state that this should correspond to the release of the coordinated water, at the beginning, and DMF molecules, later on at the thermogram. Drug molecular storage experiments revealed that the porous structure could be dosed with guaiacol molecules at a ratio of 0.19 g g^{-1}; the molecular size of guaiacol was 4.9 × 4.1 Å, which is smaller than the channel size of Ca-MOF. On the other hand, the same probes were made with ibuprofen. The TGA measurement for ibuprofen was performed as well; however, there was no obvious signal pointing to the residual of ibuprofen in the framework of Ca-MOF, since all the guest molecules in the sample were gone when the temperature was lower than 100°C. The drug release experiments were performed by guaiacol samples immersed in PBS solution (pH = 7) and the UV-Vis spectroscopy of the guaiacol release solution was monitored *in situ* for 24 h. The results showed that the guaiacol molecules were released slowly from Ca-MOF, and after 15 h the absorbance reached the maximum value, demonstrating a slow molecule release process and its potential application in medical use. Further work should explore the anionic property of the Ca-MOF, so the drug candidate would be extended from the neutral one to a cationic one, which may achieve the required drug release controlled by strong electro interaction [18].

Halloysite (Hal), a clay mineral of the kaolin group, is of great interest due to a variety of its potential applications. Many Hal nanotubes were functionalised with a polyamidoamine (PAMAM) dendrimer to obtain polyamidoamine dendrimer-functionalised halloysite nanotubes (Hal_PAMAM). These were obtained with single tube lengths between 200 and 1000 nm, the external diameter = 25–50 nm, internal diameter = 9–20 nm, these materials were characterised by FTIR, XRPD, TGA, SEM and TEM. The Hal_PAMAM was tested as a carrier of three different drugs, chlorogenic acid (CHLG), ibuprofen (IBU) and salicylic acid (SAL). The higher adsorption capacity was 123.16 mg g^{-1} for CHLG; 182.72 mg g^{-1} for IBU; 39.52 mg g^{-1} for SAL as compared to raw halloysite and 3-aminopropyltrimethoxysilane (APTS) functionalised-halloysite nanotubes. As a result of surface functionalisation of halloysite with the dendrimer, the release rate of CHLG and SAL decreased, while the release profile of IBU was like that of APTS functionalised nanotubes. The accumulative CHLG release decreased from 90% for Hal to about 55% for Hal_PAMAM, while the IBU release rates slowed down and for SAL the release rate decreased with respect to the other materials. The *in vivo* toxicity studies showed that the Hal_PAMAM had no effect on the living organisms used in the bioassays against *Acutodesmus acuminatus* and *Daphnia magna* [19].

Clay nanotubes are a nanomaterial carrier for sustained drug delivery that provide an extended 10–20 h release profile. These 50 nm diameter aluminosilicate tubes, with inner-alumina and outer-silica surface layers, could be loaded with 10–30 wt% of drug molecules, DNA and enzymes (**Figure 13**). Clay nanotubes were evaluated for the delivery of different drug types, such as the anti-cancer drug Paclitaxel (release pattern initiation after 6 h, slow release over 24 h), and anti-inflammatory drugs such as SAL (burst 89% release within; then slow rate release over 100 min) and IBU (initial burst within 10 min; slow rate release over 7 h) [20].

Novel nanohybrids have been used for the local release of drugs, particularly layered double hydroxides (LDHs), widely known as hydrotalcite-like compounds. These anionic clays are synthetic positively charged thin layer structures with exchangeable interlayer of anions. Many of these materials were synthesised with different molar ratios of Zn/Al-NO_3 and Zn/Al-CO_3 LDHs and were prepared by three different ion-exchange techniques. Three molar ratios were used: 0.3:1 to 0.5:1 and 1:1. The resulting materials were intercalated with dexamethasone (DEXA) and deposited into nanotubes of anodised titanium (ATS-NL-1D), and the resulting nanotubes were characterised using FTIR and XRPD. The incorporation of DEXA anions in LDHs increased and this fact was confirmed by a diffraction lines $d_{(003)}$ to lower Θ with a maximum spacing from 8.9 to 15.09 Å, 16.70 and 21.215 Å for the nanohybrids, with a loading capacity of 12% (**Figure 14**). The test of cell viability revealed that the material was not toxic, the value of release of material was 80% of DEXA in 800 min, and the viability was 81.8% when this material was used for bone implants [21].

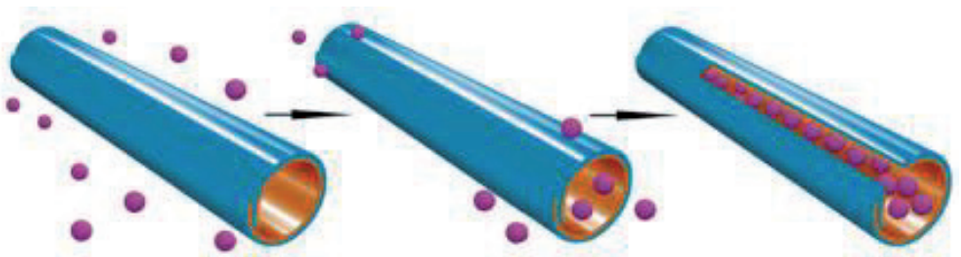

Figure 13.
Scheme of drug molecules loading into clay nanotubes [20].

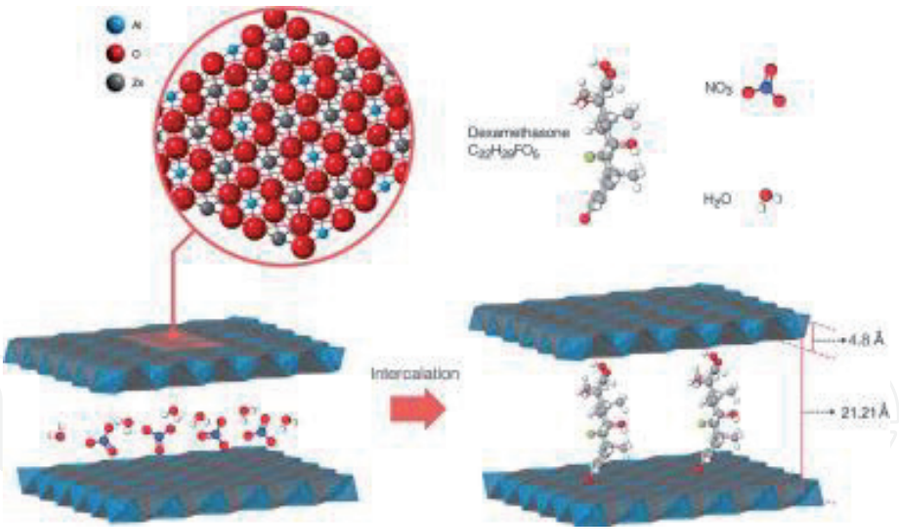

Figure 14.
Schematic illustration of the nitrate layered double hydroxide before and after intercalation of DEXA [21].

2.3 Miscellaneous

Despite the increasing interest in MOFs for biomedical applications, the development of suitable formulations for different administration ways is still a major challenge. A simple, fast and bio-friendly press-moulding method has been proposed for the obtention of cutaneous patches using composites of MIL-100(Fe). The physicochemical properties of the patches implying structure, hydration, bio adhesivity, swelling properties, as well as their encapsulation and release capabilities, both in *ex vitro* and *ex vivo* models were evaluated using different active ingredients like challenging cosmetic liporeductor, caffeine and IBU. High concentrations of caffeine were taken up for these patches with sustained releases under experimental cutaneous physiological conditions due the swelling of these devices. These patches afforded progressive and adequate permeation of their loaded molecules across the skin, reaching the adipose tissue. These characteristics make MOF-based patches as promising candidates for cosmetic applications (**Figure 15**) [22].

The Cu-BTC (BTC =1,3,5-benzenetricarboxylate) is a MOF considered the ideal porous framework in comparison with activated carbon due to its exceptional thermal and mechanical stability. The ultrasound assisted synthesis of Cu-BTC nanoparticles has been studied *vs* bulk Cu-BTC and activated carbon. To test the absorption capacity of the Cu-BTC for Rifampicin (Rif), a sample of Cu-BTC was put in an aqueous solution of Rif and the absorption was measured in real time with UV-vis technique. The samples were characterised with XRPD, SEM, FTIR and UV-vis spectroscopy. The adsorbed quantity of Rif over nano Cu-BTC (Rif@Cu-BTCNANO) was much higher (42.15 mg g^{-1}) than those over a bulk Cu-BTC (Rif@Cu-BTC) (25.62 mg g^{-1}) and activated carbon (18.85 mg g^{-1}) (**Figure 16**). In compound Rif@Cu-BTCNANO and all the nano-MOFs the channel length is decreased so that the amount of adsorption is increased a little. The delivery of Rif in ethanol increases with time, indicating that the Rif release is governed by the host-guest interaction. At 7 days of treatment, Rif release from Rif@Cu-BTCNANO, Rif@Cu-BTC and activated carbon was 78.47, 64.91 and 37.78%, respectively [23].

The direct incorporation of carboxylated carbon nanotubes (f-CNTs) into hydrophobic drug particles has been reported for the first time. The antifungal griseofulvin (GF) and the antibiotic sulfamethoxazole (SMZ) via anti-solvent precipitation, it consists that GF and SMZ were dissolved in acetone, and then added to a dispersion of f-CNTs in water, with the mixture turning cloudy when the crystals

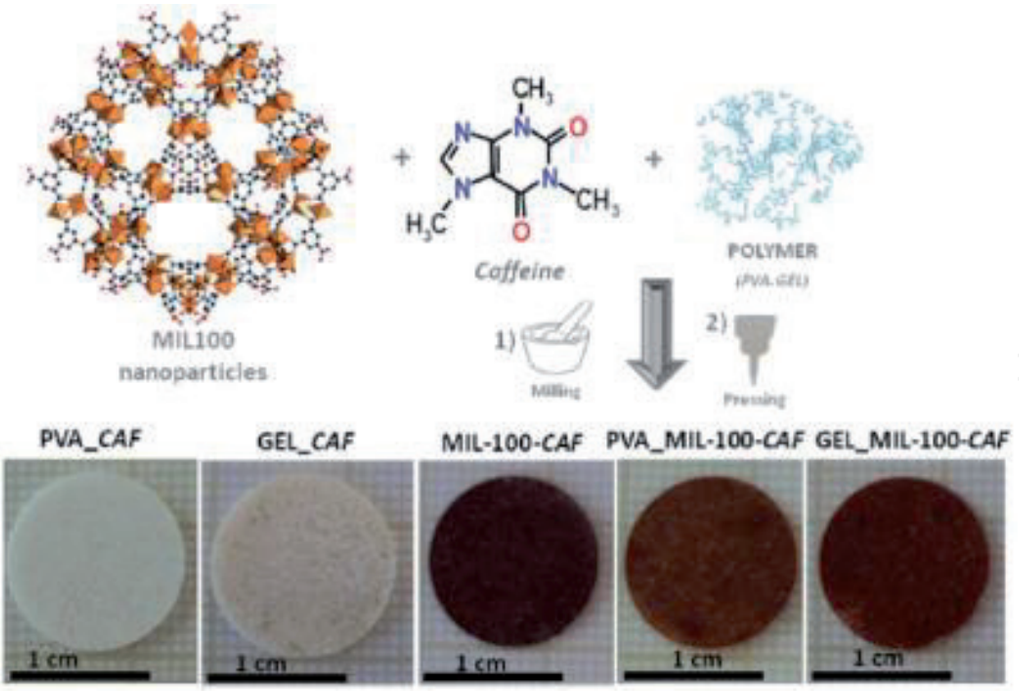

Figure 15.
Schematic view of the composite patch preparation together with images of the different obtained patches [22].

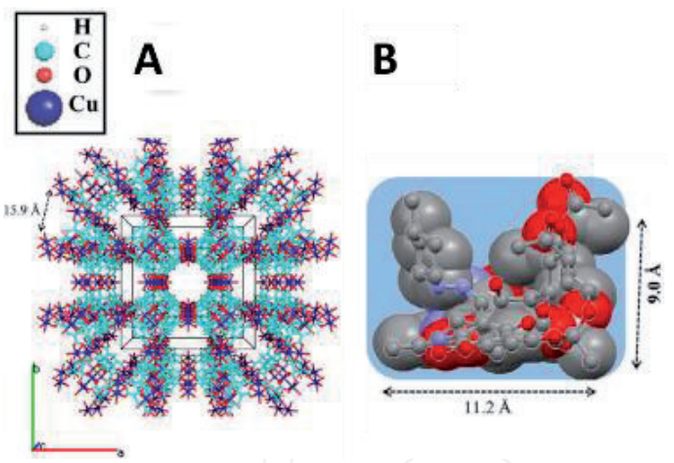

Figure 16.
(A) The pore of Cu-BTC. (B) Size of the Rif in comparison with pore size [23].

were formed. When f-CNTs were dispersed in water they acted as a nucleating site for the crystals and this fact allowed the rapid incorporation of the drug particles and increased the solubility. The time necessary to reach 80% dissolution (t_{80}) of the drugs decreased from 67 to 10 min with the incorporation of 5.1% of f-CNTs in the case of SMZ. For GF, the decrease was from 66 to 18 minutes with the addition 4% of f-CNTs (**Figure 17**) [24].

Also, there are nanotubes of carbon with cisplatin bonded that were synthesised and tested against promastigotes and amastigotes of *Leishmania major*. The cisplatin was bonded to single walled (CP-SWCNT) and multiwalled (CP-MWCNT) carbon nanotubes, and both materials were evaluated using TEM and FTIR. The value of size was between 100 and 1000 nm in the longitudinal direction, and the diameter was <10 nm and <30 nm for CP-SWCNT and CP-MWCNT, respectively (**Figure 18**). The IC_{50} obtained with CP-SWCNT was 0.39 μM and for CP-MWCNT was 0.24 μM against promastigote, while against amastigote the IC_{50} was 0.17 and 0.11 μM, respectively [25].

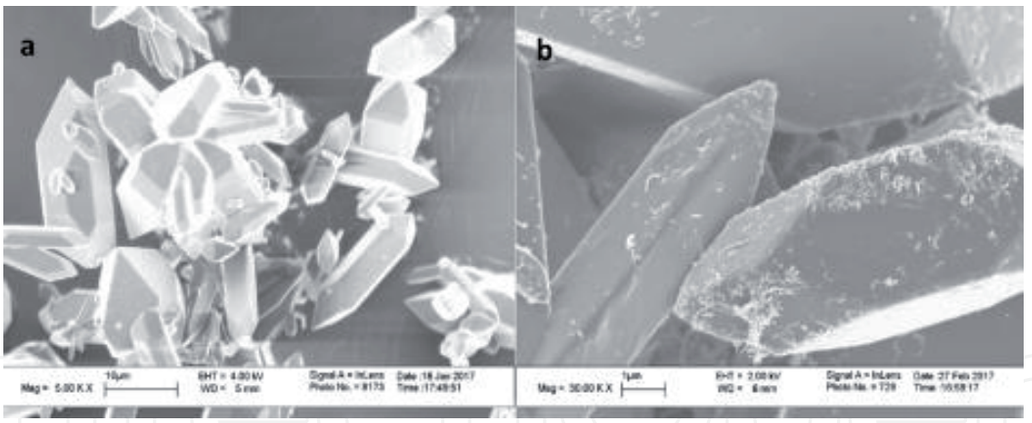

Figure 17.
SEM images of (a) GF and (b) GF-CNTs [24].

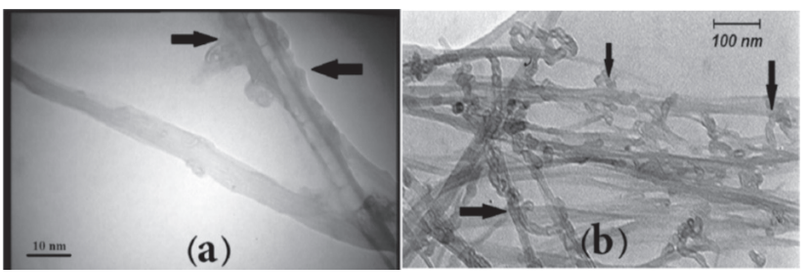

Figure 18.
TEM images of (a) CP-SWCNT and (b) CP-MWCNT [25].

Peripheral nerve injury (PNI) often results in a loss of sensory, motor, and autonomic functions in the affected region. Current treatments depend largely upon surgical intervention, most popularly the use of autografts and allografts. For that reason, the use of HNTs to form a stronger chitosan-HNT composite structure has been investigated. HNTs with biodegradable chitosan were synthesised, with interconnected, longitudinally-aligned pores with an average size of 59.3 ± 14.2 μm. This material was used for sustained delivery of 4-aminopyridine (4-AP), to improve the rate of nerve regeneration. TGA profiles indicated a 7.69 wt% overall drug loading, compared with unmodified HNTs where average load is 5–10 wt%. On the first 7 days 30 ± 2% of encapsulated drug was release (**Figure 19**). *In vivo* studies carried out in Wistar rats with a primary focus on sciatic nerve studies showed an increase in strength and mobility over a period of 4 weeks after the implantation of 4-AP. Histological evaluation demonstrated biocompatibility and regeneration of the nerve. These studies demonstrated that the development of HNTs has a high potential to improve peripheral nerve regeneration and repair [26].

Titania nanotubes (Ti-NTs) have been proven to be good drug carriers and could release drugs efficiently around implants. Enoxacin (EN), an antibiotic with the possibility to be used for anti-osteoclastogenesis, was loaded into the Ti-NTs to obtain the complex Ti-NT + EN, and then was coated with type I collagen and HA to obtain Ti-NT + EN + Col/HA, both materials were characterised by X-ray photoelectron spectroscopy (XPS) (**Figure 20**). The results indicated that the loading efficiency of EN was 75% after the initial rinse. EN release was measured by HPLC and on the 10th day the total amount of EN released by Ti-NT + EN and Ti-NT + EN + Col/HyA was 41.03 and 37.61 μg, respectively. Ti-NT + EN and Ti-NT + EN + Col/HyA were tested in the model of ovariectomised rats to evaluate the effect of osteogenesis and osteoclastogenesis. The results indicated that Ti-NT + EN + Col/HyA could promote osseointegration in ovariectomised rats better than Ti-NT + EN [27].

Figure 19.
Schematic of 4-AP drug loading into HNT, followed by sustained release of drug from lumne [26].

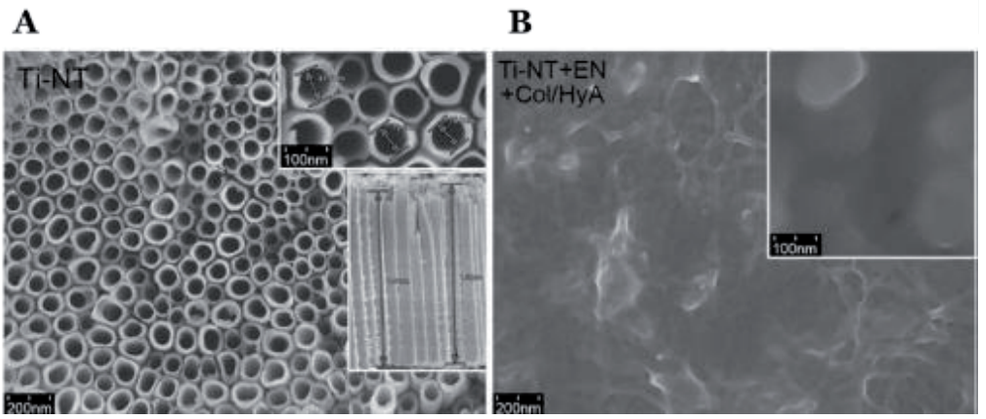

Figure 20.
SEM images of the surface morphology of (A) Ti-NT and (B) Ti-NT + EN + Col/HyA [27].

3. Biomedical applications

The HNTs have been widely used for controlled drug delivery, immobilisation of enzymes and for the capture of circulating tumour cells. These nanotubes were functionalised by two different organosilane reagents, Trimethoxy (propyl) silane (TMPS) and Triethoxy (octyl) silane (EOS), to improve their properties. Functionalisation was carried out by mixing HNTs and the organosilane reagent in acetone, and was heated at 50°C for 48 h. Both HNTs and their modifications were characterised by SEM, XRD, TGA and FTIR (**Figure 21**). The biocompatibility and cytotoxicity of these nanomaterials were determined using C6 rat glioblastoma cells. The results suggested that before being functionalised the nanotubes showed a high biocompatibility and low cytotoxicity. In contrast with their organosilane derivatives, increased cell mortality was observed after incubating under the same conditions [28].

Trichloroisocyanuric acid (TCCA) tablets are used for water treatment in swimming pools. This has been a widely used and safe way of releasing hypochlorous acid with wide biological capabilities, for instance, disinfectant, algaecide and bactericide application. The cited paper studied the incorporation of insect repellents (geranic acid, citronellic acid, geraniol and IR3535) in TCCA tablets with a simultaneous perfume/essence function. Although the mixture of TCCA with the repellents is not possible due to the incompatibility between both components, the researchers proposed a strategy of incorporation in silica and MOFs MIL-53(Al) and MIL-88A(Al) (**Figure 22**). The formulation of TCCA with the incorporated repellents resolved the incompatibility and produced a new tablet that could be used in water treatment, insect repellency and perfume [29].

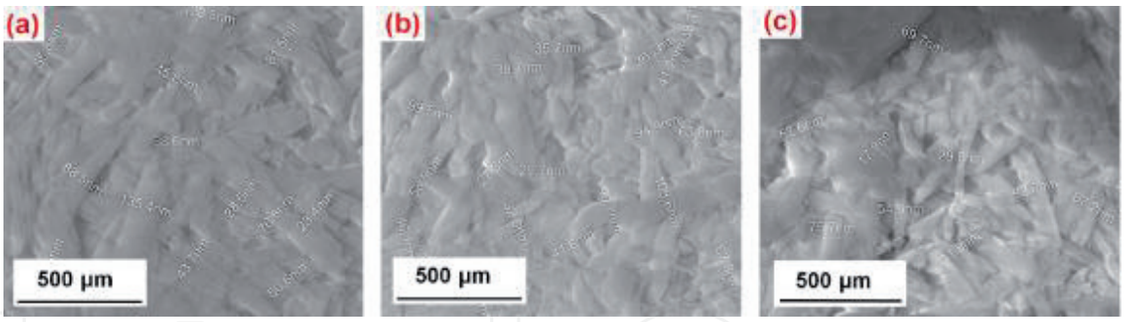

Figure 21.
SEM images of (a) HNTs, (b) HNTs-TMPS and (c) HNTs-EOS [28].

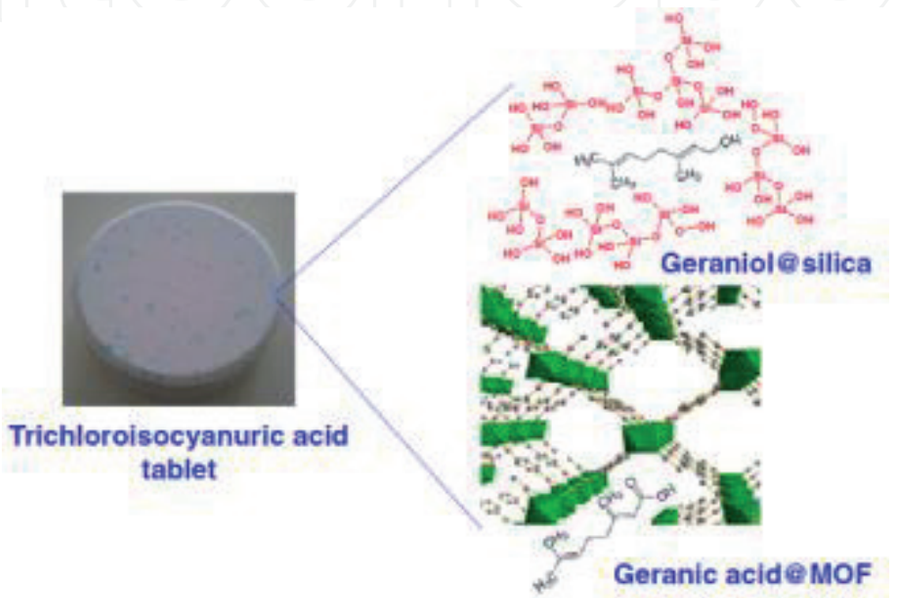

Figure 22.
Trichloroisocyanuric acid tablet [29].

In this contribution, the authors defined that a well-controlled three-step green synthetic method allowed the synthesis of composite materials based on the highly stable chromium (III) terephthalate MIL-101(Cr) MOF with Au NPs and polyoxometalates (POMs) inside its mesopores, developing (Au)POM@MOF ensembles. The strategy included, as a first step, the inclusion of POM into the MIL-101(Cr) cages by direct synthesis method of MIL-101(Cr) in the presence of $H_3PMo_{12}O_{40}$ (POM). Then, POM was reduced using H_2 and finally a soft reduction of $HAuCl_4$ was performed to obtain Au NPs and oxidised POM into the MIL-101(Cr) structure [(Au)H_2redPOM@101] (**Figure 23**). The final atomic ratio of 1.8 for Au/POM was reached. Characterisation studies revealed that the chemical and structural stabilities of both MIL-101(Cr) and the POM were preserved during the whole process. Although the crystalline structure of the MOF was pre-served, the Au NPs were successfully incorporated within the MOF and are strongly associated with the framework, as confirmed by their exceptional stability under physiological conditions (cell culture medium). These results clearly underline the potential applications of these composites to the *in situ* formation of other interesting metal NPs within the pores of MOFs. In addition to the potential physicochemical properties of these highly porous composite systems, the authors state their promising performance as optical contrast agents. The (Au)H_2red-POM@101 composites exhibited excellent biostability and were rapidly internalised in macrophage cells, as observed by fluorescence confocal microscopy. In this line, a suitable biological interaction was evidenced, as confirmed

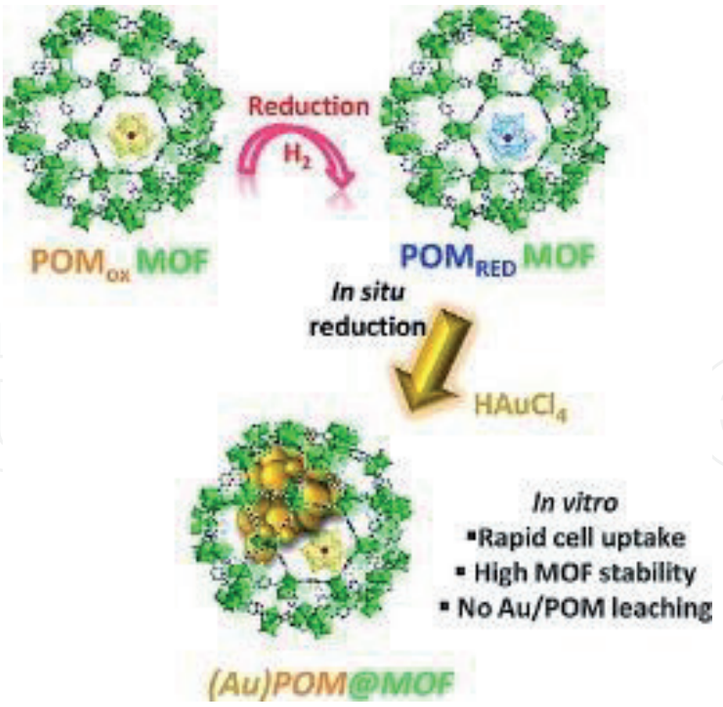

Figure 23.
Schematic representation of (Au)POM@MOF [30].

by the rapid cell internalisation of these (Au)POM@MOF composites. In addition, the previously proven important capacity to encapsulate and progressively release drugs from MOFs, together with the potential antitumoral and antiviral activity of POMs, make them interesting candidates in theranostics field [30].

In biotechnology, protein and especially enzyme immobilisation provides technical and economic advantages since the molecules could be used multiple times for the same reaction, demonstrating enhanced stability under extreme conditions of temperature, pH, salts and denaturing solvents. Therefore, they have longer half-lives since they degrade less and recover better and they are suitable for continuous processes. Conjugated protein-carbon nanotubes possess unique physicochemical properties that make them attractive to a wide range of applications. Thus, the effects of covalent conjugation of lysozymes with the activity and stability of SWCNTs were analysed. The carbodiimide method was used to coupling the lysozyme with SWCNTs (**Figure 24**). After the enzyme was analysed using fluorescence methods, plots of protein unfolding using different concentrations from 0 and 6 M of guanidine hydrochloride (Gn-HCl) were generated. Free lysozyme showed a notable increase in the fluorescence value at 287 nm, besides to a red

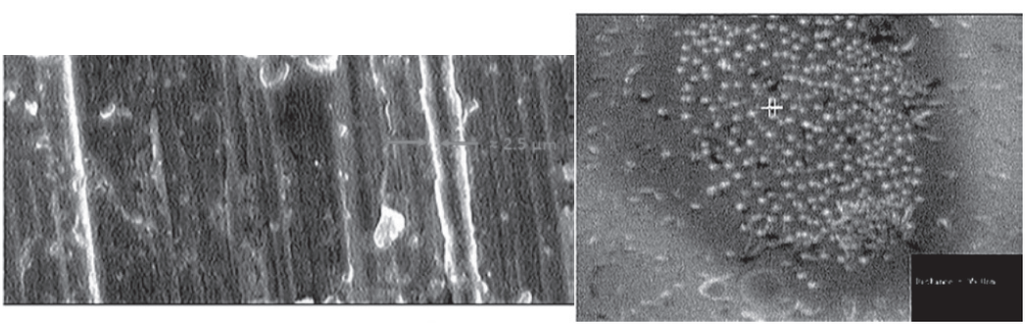

Figure 24.
SEM of conjugated lysozyme-SWCNTs (a) diameter of a bundle of lysozyme-SWCNTs = 2.5 μm, (b) average diameter of each conjugated lysozyme-SWCNTs = 95 nm [31].

shift from 343 to 352 nm. The emission spectrum of conjugated lysozyme showed a substantial increase in the fluorescence at 287 nm and an important decrease in the value at 348 nm. These results support the important role of tryptophan and phenylalanine residues in the fluorescence of conjugated and free lysozymes. Kinetic parameters were observed in KM from 4.8 to 5.6 mM and Vmax from 193 to 197 nmol min^{-1}. The conjugated lysozyme showed a notable increase in pH stability from 3.0 to 10.0 at 70°C. The inactivation kinetic showed a behaviour of first-order for free and conjugated lysozymes when they were incubated for 10 min at 70°C obtaining a value of K = 0.139 min^{-1}, in the presence of KCl and KSCN. The results of this study confirmed the excellent potential of the SWCNTs as a support for enzyme immobilisation [31].

4. Conclusions

In recent years the development of these composite materials has been grown due to their emergent biomedical applications. This 5 years survey evidenced that these materials have been employed with the intend to treat cancer, as anti-inflammatory agents, behaving as controlled-drug delivery systems or enzyme enhancers-immobilisers, and other potential applications such as theranostics, also were found intends to develop combined therapeutics like photodynamic-chemotherapy, among other applications. Some of the most featured findings in this research gathering revealed that even 2–3 orders of magnitude of efficacy have been determined for the loaded drug@material composites in comparison to the free drug state. Some other important features are that imidazolate materials resulted to be efficient drug delivery vehicles in antitumor therapy, especially in inhibiting autophagy of cancer cells. In general, it has been settled that acidic media is more feasible to release molecular contents of composites, but nevertheless this is also depending on chemical nature of composite itself, e.g. the physicochemical properties of drug as well as material confiner. Moreover, the broad applicability of these materials is just emerging, and we are going to presence very important developments in these lines in the near future.

Conflict of interest

The authors declare no conflict of interest.

DOI: http://dx.doi.org/10.5772/intechopen.89626

Author details

Miguel Martell-Mendoza[1], Cuauhtémoc Pérez-González[1], Hiram I. Beltrán[2], Roberto Serrano-Vega[1] and Carlos Alberto Méndez-Cuesta[1*]

1 Universidad Autónoma Metropolitana-Xochimilco, Mexico City, Mexico

2 Universidad Autónoma Metropolitana-Azcapotzalco, Mexico City, Mexico

*Address all correspondence to: cmendezc@correo.xoc.uam.mx

References

[1] Alshehri R, Muhammad A, Hasan A, Arnaout A, Ahmed F, Memic A. Carbon nanotubes in biomedical applications: Factors, mechanisms, and remedies of toxicity. Journal of Medicinal Chemistry. 2016;**59**:8149-8167. DOI: 10.1021/acs.jmedchem.5b01770

[2] Anand R, Borghi F, Manoli F, Manet I, Agostoni V, Reschiglian P, et al. Host-guest interactions in Fe(III)-trimesate MOF nanoparticles loaded with doxorubicin. The Journal of Physical Chemistry. B. 2014;**118**:8532-8539. DOI: 10.1021/jp503809w

[3] Rodriguez V, Maksimenko A, Anand R, Monti S, Agostoni V, Couvreur P, et al. Efficient "green" encapsulation of a highly hydrophilic anticancer drug in metal-organic framework nanoparticles. Journal of Drug Targeting. 2015;**23**:759-767. DOI: 10.3109/1061186X.2015.1073294

[4] Fumei L, Baohong L, Chunfeng W, Yongping Z, Jianqiang L, Chu-Ying G, et al. Encapsulation of pharmaceutical ingredient linker in metal–organic framework: Combined experimental and theoretical insight into the drug delivery. RSC Advances. 2016;**6**:47959-47965. DOI: 10.1039/c6ra06178h

[5] Zheng H, Zhang Y, Liu L, Wan W, Guo P, Nyström A, et al. One-pot synthesis of metal–organic frameworks with encapsulated target molecules and their applications for controlled drug delivery. Journal of the American Chemical Society. 2016;**138**:962-968. DOI: 10.1021/jacs.5b11720

[6] Vasconcelos I, Wanderley K, Rodrigues N, da Costa N, Freire R, Junior S. Host-guest interaction of ZnBDC-MOF + doxorubicin: A theoretical and experimental study. Journal of Molecular Structure. 2017;**1131**:36-42. DOI: 10.1016/j.molstruc.2016.11.034

[7] Chen X, Tong R, Shi Z, Yang B, Liu H, Ding S, et al. MOF nanoparticles with encapsulated autophagy inhibitor in controlled drug delivery system for antitumor. ACS Applied Materials & Interfaces. 2018;**10**(3):2328-2337. DOI: 10.1021/acsami.7b16522

[8] Shu F, Lv D, Song XL, Huang B, Wang C, Yu Y, et al. Fabrication of a hyaluronic acid conjugated metal organic framework for targeted drug delivery and magnetic resonance imaging. RSC Advances. 2018;**8**(12):6581-6589. DOI: 10.1039/C7RA12969F

[9] Wu Y, Yang J, Gao HY, Shen Y, Jiang L, Zhou C, et al. Folate-conjugated halloysite nanotubes, an efficient drug carrier, deliver doxorubicin for targeted therapy of breast cancer. ACS Applied Nano Materials. 2018;**1**(2):595-608. DOI: 10.1021/acsanm.7b00087

[10] Perween S, Misra A, Ramakumar S, Singh V. Self-assembled dipeptide nanotubes constituted by flexible β-phenylalanine and conformationally constrained α, β-dehydrophenylalanine residues as drug delivery system. Journal of Materials Chemistry B. 2014;**2**:3096-3106. DOI: 10.1039/c3tb21856b

[11] Azqhandi M, Farahani B, Dehghani N. Encapsulation of methotrexate and cyclophosphamide in interpolymer complexes formed between poly acrylic acid and polyethylene glycol on multi-walled carbon nanotubes as drug delivery systems. Materials Science and Engineering: C. 2017;**79**:841-847. DOI: 10.1016/j.msec.2017.05.089

[12] Hindumathi R, Jagannatham M, Haridoss P, Sharma CP. Novel nano-cocoon like structures of polyethylene glycol–multiwalled carbon nanotubes for biomedical applications. Nano-Structures & Nano-Objects.

2018;**13**:30-35. DOI: 10.1016/j.nanoso.2017.11.001

[13] Rao KM, Kumar A, Suneetha M, Han SS. pH and near-infrared active; chitosan-coated halloysite nanotubes loaded with curcumin-Au hybrid nanoparticles for cancer drug delivery. International Journal of Biological Macromolecules. 2018;**112**:119-125. DOI: 10.1016/j.ijbiomac.2018.01.163

[14] Liu X, Xu D, Liao C, Fang Y, Guo B. Development of a promising drug delivery for formononetin: Cyclodextrin-modified single-walled carbon nanotubes. Journal of Drug Delivery Science and Technology. 2018;**43**:461-468. DOI: 10.1016/j.jddst.2017.11.018

[15] Tan M, Karthivashan G, Arulselvan P, Fakurazi S, Zobir M. Sustained release and cytotoxicity evaluation of carbon nanotube-mediated drug delivery system for betulinic acid. Journal of Nanomaterials. 2014;**2014**:862148. DOI: 10.1155/2014/862148

[16] Bharath G, Rambabu K, Banat F, Anwer S, Lee S, BinSaleh N, et al. Mesoporous hydroxyapatite nanoplate arrays as pH-sensitive drug carrier for cancer therapy. Materials Research Express. 2019;**6**:085409. DOI: 10.1088/2053-1591/ab2348

[17] Deng C, Zhang Q, Fu C, Zhou F, Yang W, Yi D, et al. Template-free synthesis of chemically asymmetric silica nanotubes for selective cargo loading and sustained drug release. Chemistry of Materials. 2019;**31**:4291-4298. DOI: 10.1021/acs.chemmater.9b01530

[18] Wei L, Lu J, Li Q, Zhou Y, Tang L, Li F. A porous Ca-MOF with nano-sized $\{Ca_{11}\}$ as building unit: Structure, drug loading and release properties. Inorganic Chemistry Communications. 2017;**78**:43-47. DOI: 10.1016/j.inoche.2017.02.010

[19] Kurczewska J, Cegłowski M, Messyasz B, Schroeder G. Dendrimer-functionalized halloysite nanotubes for effective drug delivery. Applied Clay Science. 2018;**153**:134-143. DOI: 10.1016/j.clay.2017.12.019

[20] Santos AC, Ferreira C, Veiga F, Ribeiro AJ, Panchal A, Lvov Y, et al. Halloysite clay nanotubes for life sciences applications: From drug encapsulation to bioscaffold. Advances in Colloid and Interface Science. 2018;**257**:58-70. DOI: 10.1016/j.cis.2018.05.007

[21] Kamyar A, Khakbiz M, Zamanian A, Yasaei M, Yarmand B. Synthesis of a novel dexamethasone intercalated layered double hydroxide nanohybrids and their deposition on anodized titanium nanotubes for drug delivery purposes. Journal of Solid State Chemistry. 2019;**271**:144-153. DOI: 10.1016/j.jssc.2018.12.043

[22] García A, Hidalgo T, Lana H, Cunha D, Blanco M, Álvarez C, et al. Biocompatible polymer–metal–organic framework composite patches for cutaneous administration of cosmetic molecules. Journal of Materials Chemistry B. 2016;**4**:7031-7040. DOI: 10.1039/c6tb01652a

[23] Abbasi AR, Rizvandi M. Influence of the ultrasound-assisted synthesis of Cu-BTC metal-organic frameworks nanoparticles on uptake and release properties of rifampicin. Ultrasonics Sonochemistry. 2018;**40**:465-471. DOI: 10.1016/j.ultsonch.2017.07.041

[24] Chen K, Mitra S. Incorporation of functionalized carbon nanotubes into hydrophobic drug crystals for enhancing aqueous dissolution. Colloids and Surfaces B. 2019;**173**:386-391. DOI: 10.1016/j.colsurfb.2018.09.080

[25] Akhtaria J, Faridniab R, Kalanic H, Bastanid R, Fakhard M, Rezvane H, et al. Potent in vitro antileishmanial

activity of a nanoformulation of cisplatin with carbon nanotubes against *Leishmania major*. Journal of Global Antimicrobial Resistance. 2019;**16**:11-16. DOI: 10.1016/j.jgar.2018.09.004

[26] Manoukianab O, Arulb M, Rudraiahbc S, Kalajzicd I, KumbarS.Alignedmicrochannelpolymer-nanotube composites for peripheral nerve regeneration: Small molecule drug delivery. Journal of Controlled Release. 2019;**296**:54-67. DOI: 10.1016/j.jconrel.2019.01.013

[27] Li H, Nie B, Zhang S, Long T, Yue B. Immobilization of type I collagen/hyaluronic acid multilayer coating on enoxacin loaded titania nanotubes for improved osteogenesis and osseointegration in ovariectomized rats. Colloids and Surfaces B. 2019;**175**:409-420. DOI: 10.1016/j.colsurfb.2018.12.033

[28] Sánchez A, Peña L, Vidaltamayo R, Cué R, Mendoza A, Zomosa V, et al. Synthesization, characterization, and in vitro evaluation of cytotoxicity of biomaterial son halloysite nanotubes. Materials. 2014;**7**:7770-7780. DOI: 10.3390/ma7127770

[29] Paseta L, Simón-Gaudó E, Gracia F, Coronas J. Encapsulation of essential oils in porous silica and MOFs for trichloroisocyanuric acid tablets used for water treatment in swimming pools. Chemical Engineering Journal. 2016;**292**:28-34. DOI: 10.1016/j.cej.2016.02.001

[30] Roch-Marchal C, Hidalgo T, Banh H, Fischer R, Horcajada P. A promising catalytic and theranostic agent obtained through the in-situ synthesis of Au nanoparticles with a reduced polyoxometalate incorporated within mesoporous MIL-101. European Journal of Inorganic Chemistry. 2016;**2016**:4387-4394. DOI: 10.1002/ejic.201600359

[31] Borzooeian Z, Taslim M, Borzooeian G, Ghasemi O, Aminlari M. Activity and stability analysis of covalent conjugated lysozyme-single walled carbon nanotubes: Potential biomedical and industrial applications. RSC Advances. 2017;**7**:48692-48701. DOI: 10.1039/c7ra07189b